MIT Libraries | DSpace@MIT

MIT Open Access Articles

L[subscript g] = 60 nm recessed In[subscript 0.7]Ga[subscript 0.3]As metal-oxide-semiconductor field-effect transistors with Al[subscript 2]O[subscript 3] insulator

The MIT Faculty has made this article openly available. ***Please share*** how this access benefits you. Your story matters.

Citation: Kim, D.-H., J. A. del Alamo, D. A. Antoniadis, J. Li, J.-M. Kuo, P. Pinsukanjana, Y.-C. Kao, et al. "Lg = 60 Nm Recessed In0.7Ga0.3As Metal-Oxide-Semiconductor Field-Effect Transistors with Al2O3 Insulator." Appl. Phys. Lett. 101, no. 22 (2012): 223507. © 2012 American Institute of Physics

As Published: http://dx.doi.org/10.1063/1.4769230

Publisher: American Institute of Physics (AIP)

Persistent URL: http://hdl.handle.net/1721.1/85946

Version: Final published version: final published article, as it appeared in a journal, conference proceedings, or other formally published context

Terms of Use: Article is made available in accordance with the publisher's policy and may be subject to US copyright law. Please refer to the publisher's site for terms of use.

Massachusetts Institute of Technology

L_g = 60 nm recessed $In_{0.7}Ga_{0.3}As$ metal-oxide-semiconductor field-effect transistors with Al_2O_3 insulator

D.-H. Kim,[1,a)] J. A. del Alamo,[2] D. A. Antoniadis,[2] J. Li,[3] J.-M. Kuo,[3] P. Pinsukanjana,[3] Y.-C. Kao,[3] P. Chen,[1] A. Papavasiliou,[1] C. King,[1] E. Regan,[1] M. Urteaga,[1] B. Brar,[1] and T.-W. Kim[4,a)]

[1]*Teledyne Scientific Company, Thousand Oaks, California 91360, USA*
[2]*Microsystems Technology Laboratories, MIT, Cambridge, Massachusetts 02139, USA*
[3]*Intelligent Epitaxy Technology, Richardson, Texas 75081, USA*
[4]*SEMATECH, Austin, Texus 78741, USA*

(Received 23 September 2012; accepted 14 November 2012; published online 27 November 2012)

In this Letter, we report on sub-100 nm recessed $In_{0.7}Ga_{0.3}As$ metal-oxide-semiconductor field-effect transistors (MOSFETs) with outstanding logic and high-frequency performance. The device features *ex-situ* atomic-layer-deposition (ALD) 2-nm Al_2O_3 layer on a molecular-beam-epitaxy (MBE) 1-nm InP layer and is fabricated through a triple-recess process. An $L_g = 60$ nm MOSFET exhibits on-resistance (R_{ON}) = 220 Ω-μm, subthreshold-swing (S) = 110 mV/decade, and drain-induced-barrier-lowering (DIBL) = 200 mV/V at $V_{DS} = 0.5$ V, together with enhancement-mode operation. More importantly, this device displays record maximum transconductance (g_{m_max}) = 2000 μs/μm and current-gain cutoff frequency (f_T) = 370 GHz at $V_{DS} = 0.5$ V, in any III-V MOSFET technology.
© *2012 American Institute of Physics*. [http://dx.doi.org/10.1063/1.4769230]

The increasing difficulty in shrinking Si complementary-metal-oxide-semiconductor (CMOS) transistor footprint while managing power consumption and extracting improved performance threatens to bring Moore's law to a halt. At its heart, the problem is the need to reduce operating voltage and the difficulty of obtaining sufficient drain current drive. A solution to this problem appears in the use of certain III-V compound semiconductors, which are endowed with very high electron mobilities and thermal velocities (Ref. 1 and references therein). Transistors with record high frequency characteristics have been demonstrated.[2] Recently, these materials have also shown great promise for a next-generation ultra-low power and high density III-V CMOS logic technology.

In the last few years, there has been impressive progress in improving the quality of high-k dielectric/channel interfaces in III-V metal-oxide-semiconductor field-effect transistors (MOSFETs) by atomic-layer-deposition (ALD).[3–7] This makes this technology promising for future scaled III-V CMOS devices. A critical problem that has received little attention in these transistors is the source and drain resistance (R_S and R_D). In order to achieve the desired transistor I_{ON}/I_{OFF} ratio, sufficiently low R_S and R_D is essential, especially as L_g scales down to the 10 nm regime. This has to be accomplished while managing short-channel effects. To date, the best III-V MOSFET features on-resistance (R_{ON}) = 440 Ω-μm, maximum transconductance (g_{m_max}) = 1750 μs/μm and subthreshold-swing (S) = 100 mV/dec at $V_{DS} = 0.5$ V.[3] In this paper, we scale beyond this result and demonstrate $L_g = 60$ nm $In_{0.7}Ga_{0.3}As$ quantum-well MOSFETs with an equivalent-oxide-thickness (EOT) = 1.2 nm Al_2O_3/InP composite insulator fabricated through a triple-recess process that yields a very tight side recess spacing. Our enhancement-mode devices exhibit record $g_{m_max} > 2000$ μs/μm and current-gain cutoff frequency (f_T) of 370 GHz of any III-V MOSFET. These are accomplished while maintaining excellent short-channel effects, manifested by S = 110 mV/dec at $V_{DS} = 0.5$ V. Our work demonstrates the promising potential of III-V MOSFETs for future CMOS logic and sub-millimeter wave applications.

Figure 1(a) shows a cross section of our device structure. From top to bottom, the epitaxial layer structure consists of a heavily doped multi-layer cap ($In_{0.53}Ga_{0.47}As$/InP/$In_{0.53}Ga_{0.47}As$), 1-nm InP barrier, 10-nm $In_{0.7}Ga_{0.3}As$ channel, 5-nm $In_{0.52}Al_{0.48}As$ spacer, Si δ-doping, and 300-nm $In_{0.52}Al_{0.48}As$ back-barrier on an InP substrate. The measured electron Hall mobility ($\mu_{n,Hall}$) is 8000 cm^2/V s with $n_s = 1 \times 10^{12}/cm^2$ at room temperature, after removal of the heavily doped cap layers.

Device fabrication is somewhat similar to that of conventional high-electron-mobility transistors (HEMTs),[8] except for the deposition of a gate oxide prior to gate metal formation. It begins with mesa isolation and non-alloyed S/D ohmic contact with 1 μm spacing. After 20 nm SiO_2 deposition by PECVD, a fine gate pattern using a single-layer ZEP-520 A is defined by e-beam lithography. This is transferred to the passivating SiO_2 layer by CF_4 plasma. Following this, we carry out a triple-recess process, as in Ref. 8. Immediately after removing the e-beam resist, 2-nm of Al_2O_3 is deposited by ALD at 250 °C. Finally, Pd/Au metal gate is formed. In this way, devices with L_g from 60 nm to 150 nm are fabricated. Figures 1(b) and 1(c) show a SEM image after triple-recess process, and a TEM image for the cross section of an $L_g = 60$ nm device with Al_2O_3 gate insulator, respectively. The TEM image also shows a tight control of the side recess spacing (L_{side}), which is around 5 nm on each side of the gate.

Figure 2(a) shows the output characteristics of representative $In_{0.7}Ga_{0.3}As$ MOSFETs with L_g = 60 nm, 100 nm,

[a)]Authors to whom correspondence should be addressed. Electronic addresses: vtsrc3@gmail.com and TaeWoo.Kim@sematech.org.

 © 2012 American Institute of Physics

Downloaded 27 Nov 2012 to 18.62.2.225. Redistribution subject to AIP license or copyright; see http://apl.aip.org/about/rights_and_permissions

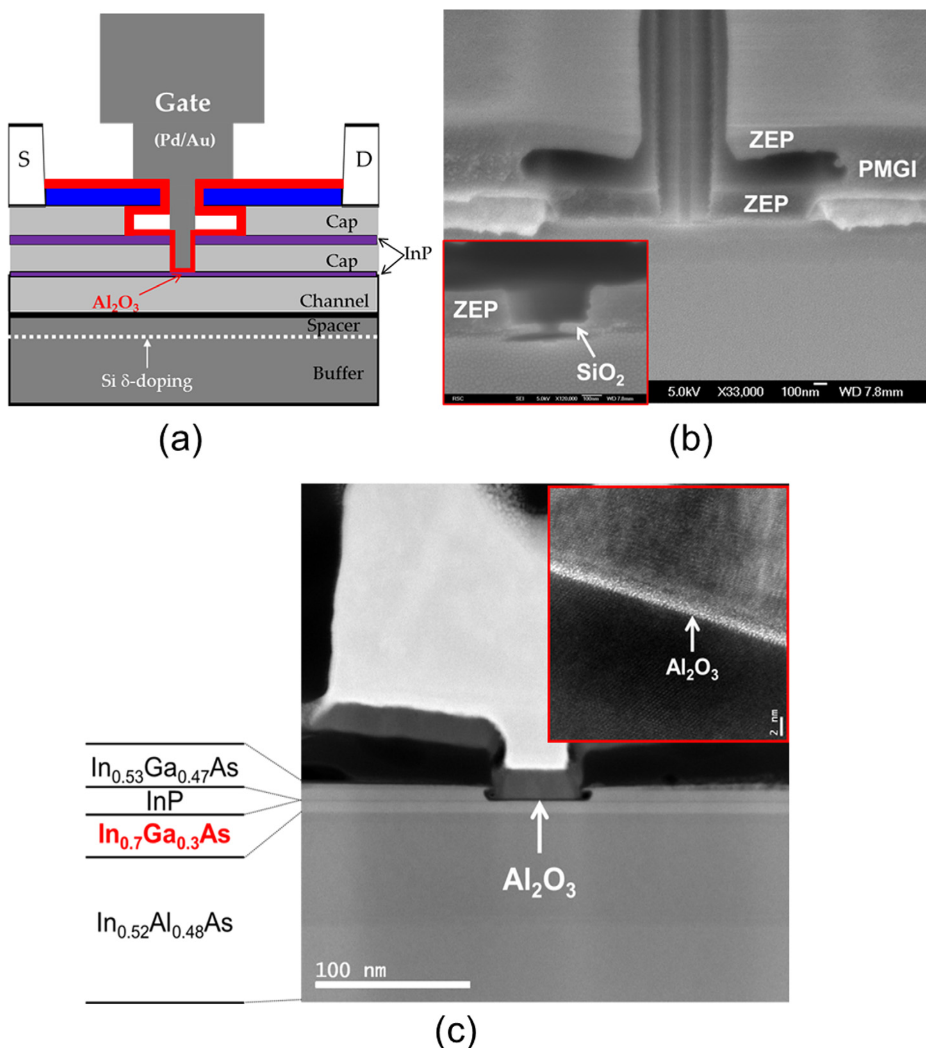

FIG. 1. (a) Schematic of recessed $In_{0.7}Ga_{0.3}As$ MOSFET with Al_2O_3 insulator, (b) SEM image before gate metallization, and (c) TEM image of the fabricated device. Physical gate length (L_g) is 60 nm and Al_2O_3 is 2-nm thick as seen in the inset of (c).

and 150 nm. The devices exhibit excellent pinch-off characteristics up to $V_{DS} = 0.5$ V, and a fairly small value of ON-resistance (R_{ON}) = 220 Ω-μm at $V_{GS} = 0.8$ V for the device with $L_g = 60$ nm. This is mainly the consequence of combining the proposed triple-recess process and the epi layer design with a multi-layer cap, which provides a tight control of the side-recess spacing ($L_{side} = 5$ nm) on each side of the gate as can be observed in the TEM image of Fig. 1(c). From transmission line method (TLM) measurements after S/D ohmic, we obtain a contact resistance (R_c) to the heavily doped cap of 15 Ω-μm and a sheet resistance (R_{sh}) of 50 Ω/sq. This outstanding value of R_{ON} yields a maximum transconductance (g_{m_max}) of 2000 μs/μm at $V_{DS} = 0.5$ V, which is the highest g_m reported in any III-V MOSFET.

Figure 2(b) shows subthreshold characteristics at V_{DS} of 0.5 V, for $L_g = 60$, 100 and 150 nm devices. Using a definition for V_T as the value of V_{GS} that yields $I_D = 1$ mA/mm, the 60 nm device exhibits enhancement-mode operation with $V_T = 0.02$ V at $V_{DS} = 0.5$ V. More importantly, the device exhibits excellent short-channel effects as manifested by a subthreshold-swing (S) of 110 mV/dec and drain-induced-barrier-lowering (DIBL) of 200 mV/V at $V_{DS} = 0.5$ V. These numbers are comparable to the device in Ref. 3, which had S = 100 mV/dec and DIBL = 130 mV/V for $L_g = 75$ nm. In addition, we find that the gate leakage current (I_G) is lower than 0.1 nA/μm at all the measured bias conditions, and that our device delivers $I_{ON} = 0.27$ mA/μm at an $I_{OFF} = 100$ nA/μm with $V_{DS} = 0.5$ V. In other words, an I_{ON}/I_{OFF} ratio is easily in excess of 10^3 in our devices, even with supply voltage of 0.5 V.

Microwave performance was characterized using a precision-network-analyzer (PNA) system with an off-wafer standard line-reflection-reflection-match (LRRM) calibration from 1 GHz to 50 GHz. We used on-wafer open and short structures to subtract pad capacitances and inductances from the measured device S-parameters. Figure 3 plots $|h_{21}|^2$, maximum-available-gain (MAG) and Mason's unilateral-gain (U_g) against frequency from 1 to 50 GHz for a 60 nm gate length device with $W_G = 2 \times 20$ μm at $V_{GS} = 0.6$ V and $V_{DS} = 0.5$ V. In this particular measurement, values of $f_T = 370$ GHz and $f_{max} = 280$ GHz were, respectively, obtained by extrapolating $|h_{21}|^2$ and U_g with a slope of −20 dB/decade using a least-squares fit. The value of f_T in our device was also verified by Gummel's approach (inset),[9] yielding $f_T = 371$ GHz. This is the highest f_T ever reported in any III-V MOSFET on any material system. In addition, it should be noted that the short-circuit current gain ($|h_{21}|^2$) keeps increasing with a −20 dB/decade slope as frequency decreases even with the positive gate bias of 0.6 V, unlike conventional HEMTs with Schottky gate. This is due to the

Downloaded 27 Nov 2012 to 18.62.2.225. Redistribution subject to AIP license or copyright; see http://apl.aip.org/about/rights_and_permissions

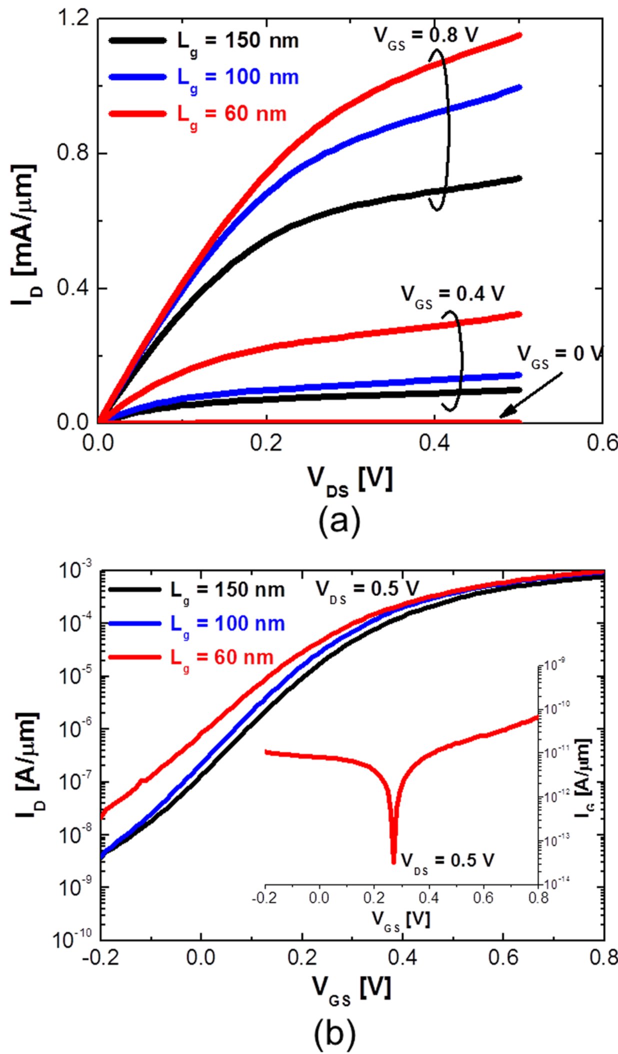

FIG. 2. DC characteristics of $In_{0.7}Ga_{0.3}As$ MOSFETs with $L_g = 150$ nm, 100 nm, and 60 nm: (a) Output characteristics and (b) subthreshold characteristics at $V_{DS} = 0.5$ V. Inset of (b) is I_G against V_{GS} for $L_g = 60$ nm device.

dramatic reduction of I_G by using the Al_2O_3 dielectric layer, as shown in the inset of Fig. 2(b).

In order to assess the significance of our work, we have benchmarked our device against reported III-V MOSFETs. From a logic operation standpoint, what matters in the end is how to maximize current driving capability at low V_{DS} while minimizing OFF-state current. As a result, both the transconductance (g_m) and subthreshold-swing (S) are of great importance, as proposed in Ref. 10. Figure 4 plots g_{m_max} as a function of S, for the devices in this work, as well as reported III-V MOSFETs with planar architectures.[3,6,7,11–13] The subthreshold-swing that we have obtained in this work is among the best reported III-V MOSFET technologies, while our g_{m_max} stands out against all of them.

Table I summarizes key device parameters for our devices in contrast with previously demonstrated $L_g = 75$ nm InGaAs MOSFET.[3] Our recessed $In_{0.7}Ga_{0.3}As$ MOSFETs combine an outstanding g_m and R_{ON}, together with excellent high-frequency response and short-channel effects down to $L_g = 60$ nm. This is mainly attributed to the triple-recess process that yields a very tight side-recess spacing ($L_{side} = 5$ nm) plus aggressive EOT scaling (EOT = 1.2 nm). This in turn suggests a very small interface density (D_{it}) below the conduction band edge, revealing that a composite dielectric stack of ALD grown Al_2O_3 and MBE-grown InP is very promising for future III-V MOSFET.

In conclusion, we have demonstrated $L_g = 60$ nm recessed $In_{0.7}Ga_{0.3}As$ quantum-well MOSFETs with EOT = 1.2 nm. The devices exhibit excellent logic characteristics, such as S = 110 mV/dec and DIBL = 200 mV/V with E-mode operation. More significantly, our devices feature record performance for any III-V MOSFET technology in terms of g_{m_max} and f_T. The outstanding performance that we demonstrate stems from the triple-recess fabrication process that yields a very tight side recess spacing, coupled with aggressive EOT scaling. Our work strongly reveals that with further device optimization in the form of self-aligned ohmic contacts, the proposed InGaAs MOSFETs with Al_2O_3 insulator could well become the technology of choice for sub-10 nm CMOS logic and THz applications.

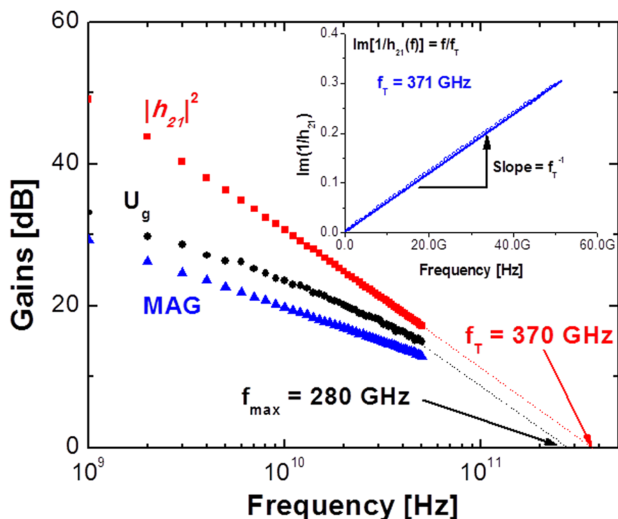

FIG. 3. $|h_{21}|^2$, Mason's unilateral-gain (U_g) and MAG against frequency for $L_g = 60$ nm $In_{0.7}Ga_{0.3}As$ MOSFET with $W_g = 2 \times 20\ \mu m$ at $V_{GS} = 0.6$ V and $V_{DS} = 0.5$ V.

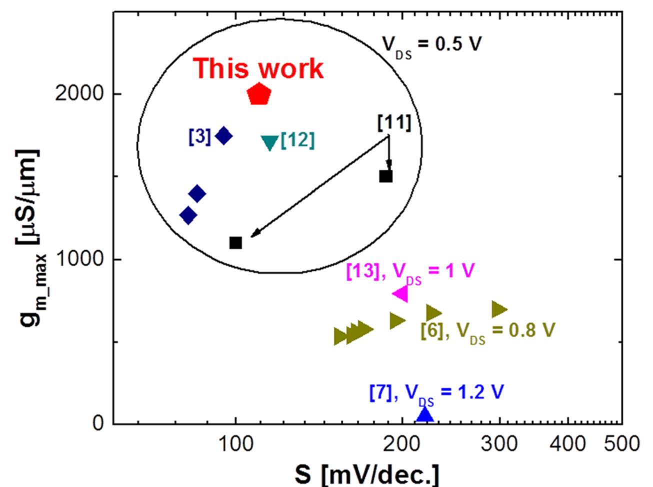

FIG. 4. Maximum transconductance (g_{m_max}) as a function of subthreshold-swing (S) for our device in this work as well as other reported III-V MOSFETs.

Downloaded 27 Nov 2012 to 18.62.2.225. Redistribution subject to AIP license or copyright; see http://apl.aip.org/about/rights_and_permissions

TABLE I. Comparison between 60 nm InGaAs MOSFET (this work) and 75 nm InGaAs MOSFET (Ref. 3) at $V_{DS} = 0.5$ V.

	L_g [nm]	EOT [nm]	R_{ON} [Ω-μm]	g_{m_max} [μs/μm]	f_T [GHz]	S [mV/dec.]	DIBL [mV/V]
InGaAs MOSFET (This work)	60	1.2	220	2000	370	110	200
InGaAs MOSFET (Ref. 3)	75	2.2	440	1750	N/A	100	130

This work was supported by the internal R&D program at Teledyne Scientific Company (TSC). The authors would like to thank Juan Paniagua, Paul Hundal, Chris Regan, and Don Deakin at TSC for help with the device fabrication. The MIT portion of this work is funded by Intel Corporation and Focus Center Research Program Center on Materials, Structures and Devices.

[1] J. A. del Alamo, Nature **479**, 317 (2011).
[2] D.-H. Kim, B. Brar, and J. A. del Alamo, Int. Electron Devices Meeting **2011**, 692.
[3] M. Radosavljevic, B. Chu-Kung, S. Corcoran, G. Dewey, M. K. Hudait, J. M. Fastenau, J. Kavalieros, W. K. Liu, D. Lubyshev, M. Metz, K. Millard, N. Mukherjee, W. Rachmady, U. Shah, and R. Chau, Int. Electron Devices Meeting **2009**, 319.
[4] M. Radosavljevic, B. Chu-Kung, S. Corcoran, G. Dewey, M. K. Hudait, J. M. Fastenau, J. Kavalieros, W. K. Liu, D. Lubyshev, M. Metz, K. Millard, N. Mukherjee, W. Rachmady, U. Shah, and R. Chau, Int. Electron Devices Meeting **2010**, 126
[5] R. Terao, Appl. Phys. Express **4**, 054201 (2011).
[6] Y. Q. Wu, W. K. Wang, O. Koybasi, D. N. Zakharov, E. A. Stach, S. Nakahara, J. C. M. Hwang, and P. D. Ye, IEEE Electron Device Lett. **30**, 700 (2009).
[7] H.-C. Chin, X. Gong, X. Liu, and Y.-C. Yeo, IEEE Electron Device Lett. **30**, 805 (2009).
[8] D.-H. Kim and J. A. del Alamo, IEEE Electron Device Lett. **31**, 806 (2010).
[9] H. K. Gummel, Proc. IEEE **57**, 2159 (1969).
[10] G. Doornbos and M. Passlack, IEEE Electron Device Lett. **31**, 1110 (2010).
[11] M. Egard, L. Ohlsson, B. M. Borg, F. Lenrick, R. Wallenberg, L.-E. Wernersson, and E. Lind, Int. Electron Devices Meeting **2011**, 303.
[12] T.-W. Kim, R. J. W. Hill, C. D. Young, D. Veksler, L. Morassi, S. Oktybrshky, J. Oh, C. Y. Kang, D.-H. Kim, J. A. del Alamo, C. Hobbs, P. D. Kirsch, and R. Jammy, Symposium on VLSI Technology Digest **2012**, 179.
[13] Y. Sun, E. W. Kiewra, J. P. de Souza, J. J. Bucchignano, K. E. Fogel, D. K. Sadana, and G. G. Shahidi, Int. Electron Devices Meeting **2008**, 367.

Downloaded 27 Nov 2012 to 18.62.2.225. Redistribution subject to AIP license or copyright; see http://apl.aip.org/about/rights_and_permissions